Rotating Nonlinear Vortical Patterns on a Gamma Plane

By Oleg G. Derzho and Brad de Young

Nonlinear barotropic vortical patterns on a γ-plane are investigated analytically. The solutions describe large-scale Rossby waves rotating anticyclonically with zero circulation. The Rossby waves are predicted to rotate with a specific angular velocity. The stream function–vorticity relation is assumed to be nonlinear, which may lead to a pronounced asymmetry within the pattern. The similarity between the simulated patterns and the Antarctic Circumpolar Wave is highlighted.

1. Introduction

In this paper, we examine the effect of rotation and the variation of the Coriolis parameter with latitude on a class of vortical structures in polar regions. A linear variation of the Coriolis parameter (the β-plane approximation) is widely used in describing many mid-latitude processes. In the polar regions, a quadratic approximation can be used to represent the Coriolis parameter (the γ-plane approximation). Rotating vortical structures with zero total circulation currently attract a great deal of attention with numerous theoretical, experimental, and observational studies (e.g., [1–4]). Our study addresses a class of vortical patterns formed by a Rossby wave with zero circulation.

We are motivated by the Antarctic Circumpolar Wave (ACW) phenomenon, a recently discovered vortical pattern rotating around the Antarctic that modifies the velocity field of the Antarctic Circumpolar Current (ACC) (e.g.,

Address for correspondence: Oleg G. Derzho, Department of Physics and Physical Oceanography, Memorial University of Newfoundland, St. John's, NL, A1B 3X7 Canada; e-mail: oderzho@mun.ca

DOI: 10.1111/j.1467-9590.2010.00502.x

STUDIES IN APPLIED MATHEMATICS 0:1–15

[3, 4]). White [5] suggested that the ACW may be part of the global El Nino-Southern Oscillation Wave and may affect climate in some parts of the Southern Hemisphere (e.g., [6]). In this paper, we model the ACW as an anticyclonically rotating Rossby wave. We also show that a cyclonic current (rotating in the contrary relative to the Rossby wave) is an inherent part of our solution.

Planetary vortices have been studied for over four decades, starting with the pioneering work by Longuet-Higgins [7]. To date, most work has focused only on understanding of dynamics of vortical structures on the β-plane (e.g., [8]). Nof [9] developed a model for modons, based on the nonlinear equations for a horizontal shallow flow on a γ-plane. The inclusion of nonlinearity allowed the author to present new modon solutions for the polar regions, which transform into the well-known solution derived by Stern for the mid-latitude case [10]. A limitation of [9] is that only nonrotating solutions were studied. Compact rotating vortex tripoles and multipoles of higher order consisting of a central vortex and a number of satellite vortices on a γ-plane were recently investigated theoretically in [11], which are similar to those observed in the pioneering experiments [2]. Fluid particles in the central core and the satellite vortices reported in [11] revolve in opposition, and the whole pattern rotates steadily. In our study, we focus on nonlinear and generally asymmetric multipole structures in a circular channel on the γ-plane.

On the technical side, our approach differs from previous studies. Theories using point vortices as a part of the construction (e.g., [1, 12]) are beyond the scope of the present paper. We classify the approaches adopted before as follows. First, there are studies on embedded finite size vortices which arise around the critical point in a shear flow. A recent analytical study employing this approach was, for example, reported in [13]. The shape of the separatrix in [13] is not prescribed *a priori* but is found as a part of the solution. Another approach relies on the circularity of the separatrix and a linear relation between streamfunction and vorticity (e.g., [9]). In [11], the streamfunction–vorticity relation is assumed to be linear in the exterior of the separatrix and nonlinear in the interior area. Here, we assume that the streamfunction–vorticity relation is nonlinear in the whole domain. We show that once a nonlinear streamfunction–vorticity relation is prescribed, it defines a set of asymmetric vortex patterns with specific amplitudes.

The paper is organized as follows. In Section 2, we formulate the equations of motion for rotating vortices on a barotropic γ-plane and identify the relevant parameters. Then, we present the derivation of an asymptotic long wave equation describing a finite amplitude vortex pattern steadily rotating in a circular channel. In Section 3, we present semi-analytical solutions of the derived equation for the particular case of vortices rotating around the Antarctic. In Section 4 some concluding remarks are offered.

2. Formulation

We consider the two-dimensional pattern of a purely barotropic fluid rotated with an angular velocity c around a geographical pole in a circular channel of the width L on a gamma plane. The dimensionless equation for the streamfunction ψ in this case is the following (e.g., [14]):

$$\left(\nabla^2\psi - \frac{\varepsilon^2}{Ro}\frac{\xi^2}{2}\right)_\phi \left(\psi - c\frac{\xi^2}{2}\right)_\xi - \left(\nabla^2\psi - \frac{\varepsilon^2}{Ro}\frac{\xi^2}{2}\right)_\xi \left(\psi - c\frac{\xi^2}{2}\right)_\phi = 0. \tag{1}$$

The streamfunction is introduced in the usual way

$$u = \psi_\xi, v\xi = -\psi_\phi, \tag{2}$$

where u, v are velocities in the eastward and the northward directions; ξ is dimensionless radial distance to the geographical pole scaled with the channel width L; and ϕ is the longitude. The dimensionless parameter ε in (1) is defined as follows:

$$\varepsilon = L/R_E \ll 1. \tag{3}$$

Thus, we consider the length scale of the flow to be much smaller than the radius of the Earth R_E. It is convenient to introduce the Rossby number in the standard form $Ro = U/2\Omega L$, where Ω is the rotation rate of the Earth and U is a typical circumferential velocity.

We use the hydrostatic approximation which is valid for sufficiently shallow (L is much greater than the oceans depth H) fluid

$$H \ll R_E\varepsilon^2. \tag{4}$$

We also assume that

$$(2\Omega L)^2/(gH) \ll 1. \tag{5}$$

It is well-known that once the latter inequality is valid, the rigid lid approximation can be used [15].

When $\psi \ll c\frac{\xi^2}{2}$ so the left-hand side of (1) is linear and only waves of small amplitudes can be described. Otherwise, $\psi \sim c\frac{\xi^2}{2}$ so the left-hand side of (1) also contains nonlinear terms.

Equation (1) can be integrated to yield

$$\nabla^2\psi - \frac{\varepsilon^2}{Ro}\frac{\xi^2}{2} = F\left(\psi - c\frac{\xi^2}{2}\right), \tag{6}$$

where F is an arbitrary function to be determined from the relation between the potential vorticity and the streamfunction at some cross sections of the flow. Classical papers such as [10] assumed that this relation is linear. We will

assume that the potential vorticity–streamfunction relation F has a weakly nonlinear functional form thus extending the classical approach. That weakly nonlinear relation was experimentally confirmed in [14].

$$F = -\lambda\left(\psi - c\frac{\xi^2}{2}\right) + \sigma^2 f\left(\psi - c\frac{\xi^2}{2}\right), \sigma \ll 1, \tag{7}$$

where λ is a constant and f determines the functional nonlinearity in the vorticity–streamfunction relation . Substitution into (6) gives

$$\frac{1}{\xi}(\xi\psi_\xi)_\xi + \frac{\psi_{\phi\phi}}{\xi^2} + \lambda\psi - \left(\frac{\varepsilon^2}{Ro} + c\lambda\right)\frac{\xi^2}{2} = \sigma^2 f\left(\psi - c\frac{\xi^2}{2}\right). \tag{8}$$

When $\sigma = 0$, the specific choice (7) for F in (6) leads to a linear equation for the streamfunction even if its amplitude is not small and all nonlinear terms on the left hand side of (1) are retained. Here, we focus on the solutions of (8) whose radial variations appear at much shorter scales compared to the angular one

$$\psi = \psi(\xi, \Phi), \Phi = \delta\phi, \delta \ll 1. \tag{9}$$

Thus (8) now reads

$$\frac{1}{\xi}(\xi\psi_\xi)_\xi + \frac{\delta^2\psi_{\Phi\Phi}}{\xi^2} + \lambda\psi - \left(\frac{\varepsilon^2}{Ro} + c\lambda\right)\frac{\xi^2}{2} = \sigma^2 f\left(\psi - c\frac{\xi^2}{2}\right). \tag{10}$$

We seek asymptotic solutions of (10) in the form of power series in the small parameter δ,

$$\psi = \psi^{(0)}(\xi, \Phi) + \delta^2\psi^{(1)}(\xi, \Phi) + \cdots \tag{11}$$

We look for solutions of (10) in a circular channel with inner and outer rigid boundaries located at $\xi = R_1$ and $\xi = R_2$, respectively, thus boundary conditions are

$$\psi_\Phi(R_1, \Phi) = 0, \psi_\Phi(R_2, \Phi) = 0, \psi(\xi, \Phi) = \psi(\xi, \Phi + 2\pi\delta). \tag{12}$$

It can be shown that the regular zeroth order solution of (8) satisfying the boundary conditions (12) has the form

$$\psi^{(0)} = \left(\frac{\xi^2}{2} - \frac{2}{\lambda}\right)\left(\frac{\varepsilon^2}{\lambda Ro} + c\right) + A(\Phi)W(\xi), \tag{13}$$

$$W(\xi) = J_0(\sqrt{\lambda}\xi)Y_0(\sqrt{\lambda}R_1) - J_0(\sqrt{\lambda}R_1)Y_0(\sqrt{\lambda}\xi), \tag{14}$$

$$J_0(\sqrt{\lambda}R_2)Y_0(\sqrt{\lambda}R_1) - J_0(\sqrt{\lambda}R_1)Y_0(\sqrt{\lambda}R_2) = 0, \tag{15}$$

where the function A in (13) is yet to be determined. The constant λ can be determined from Equation (15) for given values R_1 and R_2.

The specific choice of the angular velocity of rotation in the form

$$c_s = -\frac{\varepsilon^2}{Ro\lambda}, \tag{16}$$

eliminates the part of the solution (13), which is independent of the longitude. Thus, the specific choice (16) eliminates a mean zeroth order current in our solution. Extension to the case with non-zero zeroth order mean current is quite straightforward and will be presented elsewhere.

The first-order equation reads

$$\frac{1}{\xi}\frac{\partial}{\partial\xi}\left(\xi\frac{\partial\psi^{(1)}}{\partial\xi}\right) + \lambda\psi^{(1)} + \frac{1}{\xi^2}\frac{\partial^2\psi^{(0)}}{\partial\Phi^2} = \frac{\sigma^2}{\delta^2} f\left(\psi^{(0)} - c_s\frac{\xi^2}{2}\right). \tag{17}$$

The requirement that all terms in the latter equation have to be of the same order leads to the scaling

$$\delta = \sigma, c_s = O(1). \tag{18}$$

Equation (17) is to be solved along with the boundary conditions (12) applied to the first-order streamfunction.

Re-writing (17) in a self-adjoint form and applying the Fredholm alternative (solvability condition) yield the equation for the amplitude function $A(\Phi)$

$$A_{\Phi\Phi}\int_{R_1}^{R_2}\frac{W(\xi)^2}{\xi}d\xi = \int_{R_1}^{R_2}\xi W(\xi) f\left(A(\Phi)W(\xi) - c_s\frac{\xi^2}{2}\right)d\xi. \tag{19}$$

Equations (13) and (19) define the streamfunction in the leading order and are the principal theoretical result of the present study.

3. Results

Let us choose f in the form of a quadratic polynomial,

$$f(B) = s_1 B + s_2 B^2. \tag{20}$$

This choice of the relationship between vorticity and streamfunction is just a straighforward extension beyond a linear relationship usually used by many authors (e.g., [10]).

This choice of f reduces (19) to the Korteveg–de Vries type equation for the wave amplitude,

$$A_{\Phi\Phi} = I_0 + AI_1 + A^2 s_2 I_2, \tag{21}$$

$$I_0 = s_1 c_s I_{01} + s_2 c_s^2 I_{02}, \tag{22}$$

$$I_{01} = \frac{-\int_{R_1}^{R_2} \frac{\xi^3}{2} W(\xi)\, d\xi}{\int_{R_1}^{R_2} \frac{W(\xi)^2}{\xi} d\xi}, \; I_{02} = \frac{\int_{R_1}^{R_2} \xi W(\xi) \frac{\xi^4}{4} d\xi}{\int_{R_1}^{R_2} \frac{W(\xi)^2}{\xi} d\xi}, \tag{23}$$

$$I_1 = s_1 I_{10} + s_2 c_s I_{11}, \tag{24}$$

$$I_{10} = \frac{\int_{R_1}^{R_2} \xi W(\xi)^2 d\xi}{\int_{R_1}^{R_2} \frac{W(\xi)^2}{\xi} d\xi}, \; I_{11} = \frac{-\int_{R_1}^{R_2} W(\xi)^2 \xi^3 d\xi}{\int_{R_1}^{R_2} \frac{W(\xi)^2}{\xi} d\xi}, \tag{25}$$

$$I_2 = \frac{\int_{R_1}^{R_2} \xi W(\xi)^3 d\xi}{\int_{R_1}^{R_2} \frac{W(\xi)^2}{\xi} d\xi}. \tag{26}$$

We can integrate (21) once assuming (without loss of generality) that $A_\Phi(\Phi = 0) = 0$, $A_0 = A(\Phi = 0)$;

$$-\frac{3}{2 s_2 I_2} A_\Phi^2 = (A_0 - A)(A - A_1)(A - A_2), \tag{27}$$

where

$$A_1 = \frac{-A_0}{2} - \frac{3 I_1}{4 I_2 s_2} - \sqrt{\left(\frac{-A_0}{2} - \frac{3 I_1}{4 I_2 s_2}\right)^2 - A_0^2 - \frac{3 I_1}{2 I_2 s_2} A_0 - \frac{3 I_0}{s_2 I_2}}, \tag{28}$$

$$A_2 = \frac{-A_0}{2} - \frac{3 I_1}{4 I_2 s_2} + \sqrt{\left(\frac{-A_0}{2} - \frac{3 I_1}{4 I_2 s_2}\right)^2 - A_0^2 - \frac{3 I_1}{2 I_2 s_2} A_0 - \frac{3 I_0}{s_2 I_2}}. \tag{29}$$

It is worth noting that $A_1 < A_0 < A_2$.

In this paper, we are looking for patterns with zero circulation, which implies that

$$\int_0^{2\pi\delta} A(\Phi)\, d\Phi = 0. \tag{30}$$

Periodicity of our problem (latter equation in the set (12)) requires that the wavelength (in radians) of the cnoidal wave is to be $\frac{2\pi\delta}{N}$. General analysis of

(21) along with (30) leads to the expression for the wavelength,

$$\frac{2\pi\delta}{N} = \frac{4K(m)}{\sqrt{A_1 - A_2}}\sqrt{\frac{-3}{2s_2 I_2}}, \tag{31}$$

$$m = \frac{A_1 - A_0}{A_1 - A_2}, \tag{32}$$

where $N = 1, 2, 3...$ is a mode number, $K(m)$ is the complete elliptic integral of the first kind.

It can be shown that all characteristics of cnoidal waves with a wavelength $\frac{2\pi\delta}{N}$ can be expressed in terms of m and N,

$$\delta^2 A_H = \frac{-6mK^2(m)N^2}{\pi^2 s_2 I_2}, \tag{33}$$

$$\delta^2 c_s = \frac{4K^2(m)N^2}{\pi^2 s_2 I_{11}}\left(2 - m - \frac{3E(m)}{K(m)}\right) - \frac{\delta^2 s_1 I_{10}}{s_2 I_{11}}, \tag{34}$$

$$\delta^2 A_0 = \frac{-6K^2(m)N^2}{\pi^2 s_2 I_2}\left(1 - m - \frac{E(m)}{K(m)}\right), \tag{35}$$

where $A_H = A_1 - A_0$ is the height of the cnoidal wave (difference between the amplitudes corresponding to the crest and to the trough). $E(m)$ is the complete elliptic integral of the second kind. It is important that m cannot be chosen arbitrarily, but rather should be defined from (32), (28), (35), (34). After some algebra, we arrive at the equation for m,

$$Q_1(R_1, R_2, m) + \frac{\delta^4 s_1^2}{N^4} Q_2(R_1, R_2) + \frac{\delta^2 s_1}{N^2} Q_3(R_1, R_2, m) = 0, \tag{36}$$

where

$$Q_1(R_1, R_2, m) = \frac{3K^4(m)}{I_2\pi^4}\left[\frac{12K^2(m)}{E^2(m)} - 4(m-1) + 8(m-2)\frac{E(m)}{K(m)} - \frac{16}{3}\frac{I_{02}I_2}{I_{11}^2}\left(2 - m - \frac{3E(m)}{K(m)}\right)^2\right], \tag{37}$$

$$Q_2(R_1, R_2) = \frac{I_{10}}{I_{11}}\left(\frac{I_{02}I_{10}}{I_{11}} - I_{01}\right), \tag{38}$$

$$Q_3(R_1, R_2, m) = -\frac{4K^2(m)\left(2 - m - \frac{3E(m)}{K(m)}\right)}{I_{11}\pi^2}\left(\frac{2I_{02}I_{10}}{I_{11}} - I_{01}\right). \tag{39}$$

Once s_1 and s_2 are set, so (36), and (37), (38), (39) determine m, which in turn determines A_0, A_H, and c_s using the relations (35), (33), and (34), respectively. It is clear that solutions to this problem (31) can exist only if $s_2 < 0$. Here, we set $s_2 = -1$ and as in the final dimensional expressions for the velocity field the key parameter is σ, the scale in the streamfunction–vorticity relation, and s_2 only appears in the product $s_2\sigma$ (or equally $s_2\delta$).

Equation (27) has solutions in the form of cnoidal waves with the wavelength $\frac{2\pi}{N}$ (for the original angular coordinate ϕ)

$$A(\phi, t) = A_0 + A_H Cn^2\left[2K(m)\frac{N}{2\pi}(\phi - c_s t)\right], \tag{40}$$

where Cn is the Jacobi elliptic function of the index m. It is straightforward to show that the specific choice of N corresponds to a $2N$-pole, that is a vortex pattern with $N = 1$ is a dipole, with $N = 2$ is a quadrupole, etc. Also, waves with small m correspond to nearly sinusoidal $A(\phi)$, the case $m = 0$ is indeed exactly sinusoidal. Vortex patterns are only marginally asymmetric for small m, the case $m = 0$ corresponds to the exact symmetry. As m increases, the wave tends to be more asymmetric which leads to the fact that one vortex (in a dipolar solution) has larger angular extent compared to another vortex. As m approaches 1, the whole vortex pattern becomes strongly asymmetrical. The limiting case $m = 1$ corresponds to a solitary wave solution for $A(\phi)$; it is clear that the case $m = 1$ cannot be reached as $A(\phi)$ has the finite period of 2π.

Here, we present our calculations for the special case of a vortical pattern rotating around the Antarctic aimed at explaining some features of the ACW. Our physical assumption is that the Subantarctic front (SAF) and the Polar Front (PF), which are reasonably well-defined narrow jets (about 40 km wide) create a wave guide for a Rossby wave. Gille [16] analyzed GEOSAT altimeter data and presented the mean paths of the SAF and PF jets. Although topography affects these paths, they stay quite close together around the Antarctic continent. According to figure 9 from [16] we estimate that the distance between SAF and PF is about 250–300 km. We model SAF and PF paths as two circumferences, which act as rigid boundaries for the Rossby wave thus creating a circular channel. We choose these internal and external circumferences at which the radial velocity is zero to be located at 3500 km and 3760 km from the South pole, respectively. We set the typical length scale to be $L = 260$ km. This means that the positions of the internal and external circumferences (in the dimensionless radial coordinate ξ) are $R_1 = 13.462$ and $R_2 = 14.462$. It can be readily checked that for the chosen length scale the condition (5) for the rigid lid approximation is justified. We set $\delta = \sigma = 0.3$, these parameters affect the magnitude of the velocity field in the wave for given s_1. We will show below that this choice of parameters leads to a reasonable agreement with observations . The period of rotation of

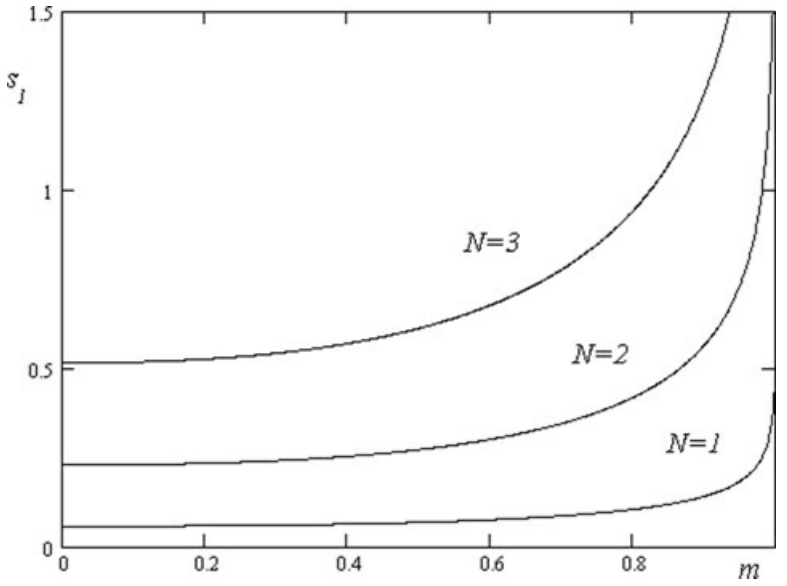

Figure 1. The graph of s_1 versus m for mode numbers $N = 1, 2, 3$.

the vortical pattern (Rossby wave) is, however, independent of the specific coefficient σ in the streamfunction–vorticity relation (7).

Using the chosen scales, and with the help of (15), (22), (24), and (26) we now can calculate λ, I_{01}, I_{02}, I_{10}, I_{11}, and I_2. The dimensional angular velocity of rotation of the vortical pattern can be calculated using (16),

$$c_{s,dim} = -\frac{L^2}{R_E^2}\frac{2\Omega}{\lambda}. \tag{41}$$

Using (41) we predict that the period of rotation of the whole structure (time to circumferent the globe) to be $T_{\text{rotation}} = 8.191$ years, which is close to the observed values reported in [3] and [17] who suggested a value of $8 - 9$ years during 1985–1994.

Once the circumferences R_1 and R_2 (at which the radial velocities are zero) are prescribed, it is straightforward to analytically determine possible values of s_1 for which stationary rotating vortex patterns exist as a function of m using the quadratic Equation (37). Only one root of the solution leads to the negative values of c_s, as only negative c_s are consistent with (16), (18). The graph of s_1 versus m (Figure 1) shows that there is a threshold for s_{1*} at each mode number N, which again can be analytically determined using (37),

$$s_{1*} = \frac{N^2}{\sigma^2}\frac{I_{02}}{I_{01}I_{11} - I_{10}I_{02}}. \tag{42}$$

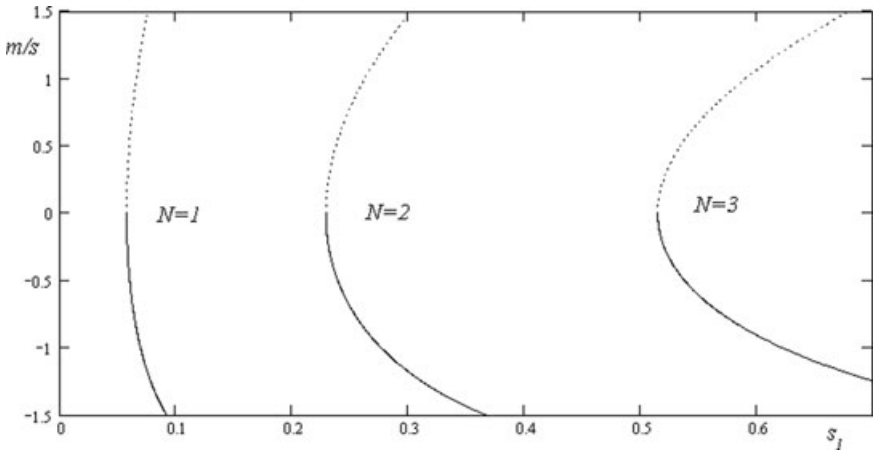

Figure 2. Maximum and minimum dimensional circumferential velocities at the outer circumference versus s_1 for mode numbers $N = 1, 2, 3$.

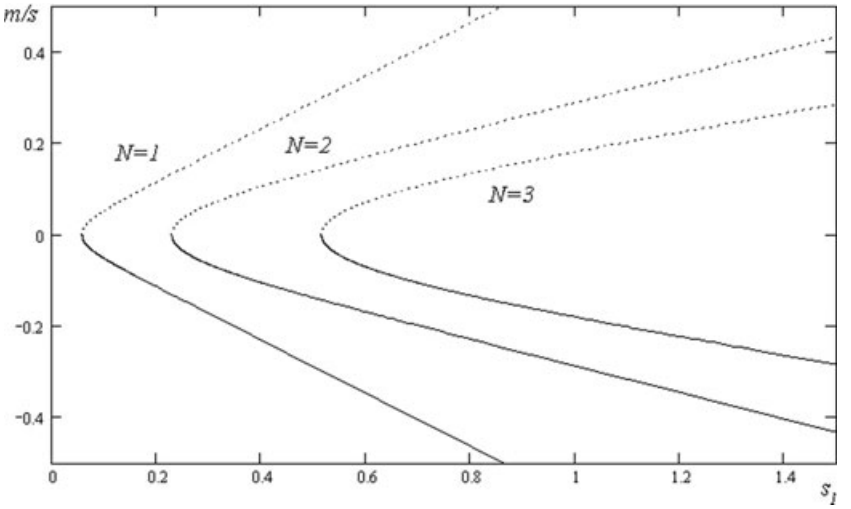

Figure 3. Maximum and minimum dimensional radial velocities at the outer circumference versus s_1 for mode numbers $N = 1, 2, 3$.

The threshold values of $s_{1*} = s_1(m = 0)$correspond to a sinusoidal (and perfectly symmetric) pattern. In our case $s_{1*} = 0.0572N^2$. Actually the pattern with $m = 0$ does not exist as its amplitude is exactly zero, and consequently the corresponding velocity field is then zero everywhere. In Figures 2 and 3 we present the maximum and the minimum of the dimensional circumferential (at the outer circumference) and radial velocities versus s_1 for various mode numbers $N = 1, 2, 3$.

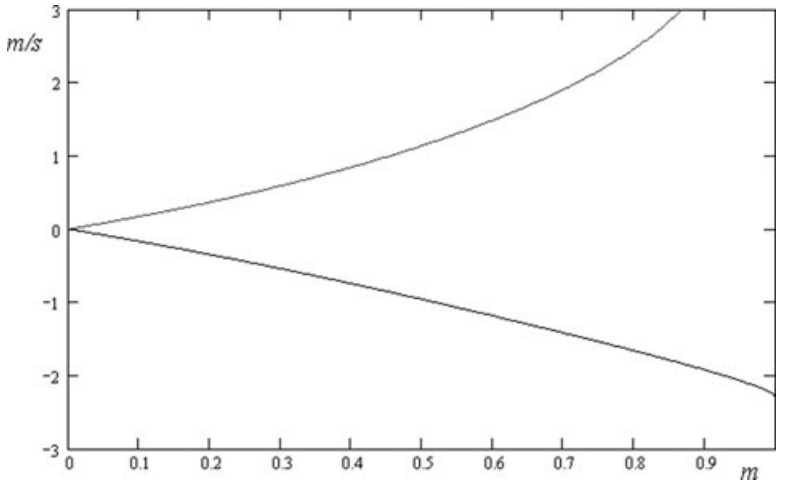

Figure 4. Maximum and minimum of the circumferential velocity as a function of cnoidal wave index m.

Geometry and all other parameters are the same as in Figure 1. These maximum velocities can be found using the expressions (13), (16), and (40) along with (2). It can be shown that maximum radial velocity occurs at $R_{\max,\mathrm{rad}} = 13.951$ (3627 km in the dimensional form) and when the value of $|dA/d\phi|$ has the maximum. Maximum and minimum radial velocities are of the same magnitude. The maximum and minimum of the circumferential velocity at $R = R_2$ occur at $A = A_0$ and $A = A_1$. It is interesting to note that maximum and minimum of the circumferential velocity as a function of cnoidal wave index m are both independent on the mode number N (see Figure 4).

Again, we recall that the leading order streamfunction patterns can be found from (13), (16), and (40). These patterns are shown in Figures 5 and 6 for the cases of dipole ($N = 1$) and quadrupole ($N = 2$); $s_1 = 0.23$ for both cases.

For the case where $N = 2$, the maximum and the minimum of the circumferential velocity at $R = R_2$ are 0.189 m/s and -0.183 m/s, respectively. The magnitudes of the circumferential velocity at $R = R_1$ are similar. Magnitude of the radial velocity ($N = 2$) is 0.009 m/s. As can be seen from Figures 2 and 3, mode $N = 1$ vortical structure (dipole) has significantly greater velocities for the case $s_1 = 0.23$, circumferential velocity reaches 4.98 m/s, and radial velocity reaches 0.132 m/s. That is for the examined vorticity–streamfunction relation, the only mode 2 structure is realizable.

Cnoidal wave indexes corresponding to the vortex patterns with $N = 1, 2, 3$ decrease as N increases: $m(N = 1) = 0.97453$; $m(N = 2) = 0.10884$; $N = 3$ mode does not exist at $s_1 = 0.23$. For $N = 1$ the pattern is asymmetric (angular extent of the smaller vortex is 133.1 degrees compared to 226.9 degrees for the larger vortex); for $N = 2$ pattern is only slightly asymmetric (angular extent of

Figure 5. Streamline pattern for the case of dipole ($N = 1$); $s_1 = 0.23$.

the smaller pair of vortices is 89.17 degrees compared to 90.83 degrees for the larger pair). The angular extent (in radians) of the smaller vortex for the case $N = 1$ is shown in Figure 7. To re-calculate for a different mode number N, the result for $N = 1$ should be divided by N.

Here, we modeled the ACW as a nonlinear Rossby wave with zero circulation. The ACW is observed to propagate against the ACC. Our theory is also capable to predict the existence of such "counter-rotating" current. Let us consider solutions of the first-order Equation (18); they consist of a general solution and particular solutions. Important observation is that the general solution and the part of the particular solution proportional to A or $A_{\Phi\Phi}$ describe a correction to the Rossby wave with zero circulation. Another part of the particular solution $\psi_C^{(1)}$ describes a current. That part obeys the following equation:

$$\frac{1}{\xi}\frac{\partial}{\partial\xi}\left(\xi\frac{\partial\psi_C^{(1)}}{\partial\xi}\right)+\lambda\psi_C^{(1)}=-s_1c_s\frac{\xi^2}{2}+s_2c_s^2\frac{\xi^4}{4}+s_2A^2(\Phi)W^2(\xi). \quad (43)$$

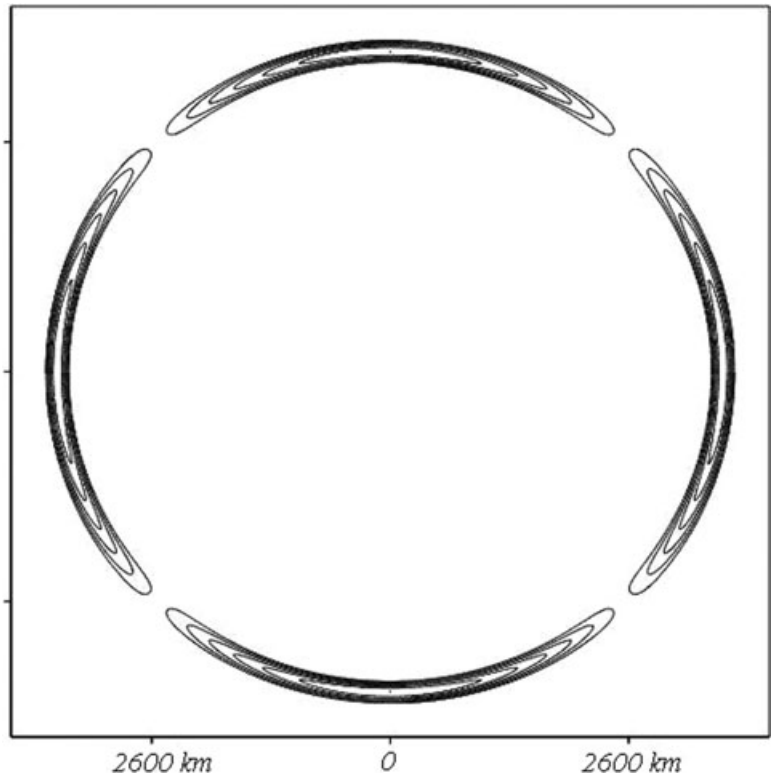

Figure 6. Streamline pattern for the case of quadrupole ($N = 2$); $s_1 = 0.23$.

The last term in the right-hand side of (43) is small compared to the first and second terms because of the large values of ξ, so for the ACW conditions the current is not much affected by the ACW and variation of the ACC with time is weak. The magnitude and spatial variation of the current depends on the boundary conditions. Extensive examination of these features is beyond the scope of the present paper, although we noticed that the direction of the current is always opposite to the sense of rotation of the Rossby wave if that eastward current direction takes place at least at one of the boundaries of the circular channel.

4. Conclusion

In this paper, we have presented a model for polar eddies in a circular domain. The case of a ring-like strip is considered in detail. The structures examined are actually Rossby waves of finite amplitude. Here, we do not impose the small amplitude approximation at all. Small amplitude Rossby waves can rotate at any angular velocity while finite amplitude ones (in order to be trapped near

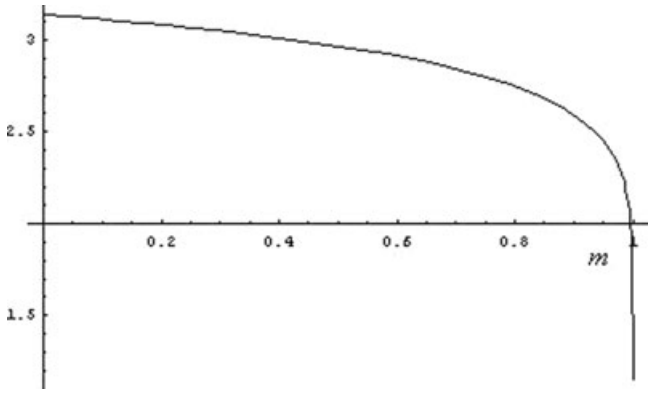

Figure 7. The angular extent, in radians, of the smaller vortex for the case $N = 1$.

the pole or trapped between the prescribed circumferences) need to rotate at some specific rate c_s, which is specified in our theory. The gamma effect is of crucial importance for the wave patterns presented in this work. To keep our finite amplitude patterns trapped they should rotate at a particular angular velocity which is defined by the gamma effect to eliminate a nonvanishing monopole component. Further, once the vorticity–streamfunction relation is prescribed, there is a unique nonlinear vortex pattern for each mode number N that satisfies the angular symmetry ($2\pi/N$ angular periodicity) of the problem. For a quadratic relation between vorticity and streamfunction, the vortex pattern has a separate dependence in the radial and the angular coordinates. We assume that the angular coordinate is a "slow" variable compared to the "fast" radial coordinate. If the length scale L, and any two circumferences at which the radial velocity is zero are prescribed, the period of rotation (time to circumferent the globe) of the whole vortical structure can be calculated using (41). The period of time required to repeat the relative position of vortices within the structure, T_{obser}, is the period of rotation divided by N, i.e., $T_{\text{obser}} = T_{\text{rotation}}/N$. Once the particular form of the vorticity–streamfunction relation (20) is specified, the wave index m determining the spatial structure of the vortices can be calculated using (37). For a given wave number N, there is only one nonlinear and asymmetric wave pattern which satisfies the formulation of the problem. If we take the size of the inner and outer circles to be 3500 and 3760 km (scales that correspond to the Subantarctic front (SAF) and the Polar Front (PF) in the Antarctic), so the maximum velocity within the pattern is about 0.2 m/s if we choose $s_1 = 0.23$. The predicted mode 2 wave (quadrupole) is slightly asymmetric. We calculated that $c_{s,dim} = -3.345 \times 10^{-4}\Omega$ corresponds to a period of propagation around the globe of about 8 years. The minus sign indicates that the vortex rotates anticyclonically. For these parameters, the maximum circumferential velocity will be 0.2 m/s. Sarukhanyan [18]

observed similar velocities in the ACC. There is therefore reasonable agreement with observed features of the Antarctic Circumpolar Wave in spite of our highly idealized approach. A more detailed examination of importance of the bathymetry and coastal configuration features would require a spatially explicit numerical model, which is beyond the scope of the present study.

References

1. H. Aref and M. A. Stremer, Four-vortex motion with zero total circulation and impulse, *Phys. Fluids* 12:3704–3715 (1999).
2. G. J. F. van Heijst, R. C. Kloosterziel, and C. W. M. Williams, Laboratory experiments on tripolar vortices in a rotating fluid, *J. Fluid Mech.* 225:301–331 (1991).
3. W. B. White and R. G. Peterson, An antarctic circumpolar wave in surface pressure, temperature and sea-ice extent, *Nature* 380:699–702 (1996).
4. G. A. Jacobs and J. L. Mitchell, Ocean circulation variations associated with the antarctic circumpolar wave, *Geophys. Res. Let.* 23(21):2947–2950 (1996).
5. W. B. White, S. C. Chen, R. J. Allan, and R. C. Stone, Positive feedbacks between the antarctic circumpolar wave and the global el nino-southern oscillation wave, *J. Geophys. Res.* 107(C10):3165–3175 (2002).
6. W. B. White and N. J. Cherry, Influence of the antarctic circumpolar wave on New Zealand temperature and precipitation during autumn-winter, *J. Climate* 12:960–976 (1998).
7. M. S. Longuet-Higgins, Planetary waves on a rotating sphere, *Proc. Roy. Soc. Lon.* A279:446–473 (1964).
8. G. Sutyrin and X. Carton, Vortex interaction with a zonal Rossby wave in a quasi-geostrophic model, *Dyn. Atmos. Oceans* 41(2):85–102 (2006).
9. D. Nof, Modons and monopoles on a γ-plane, *Geophys. Astroph. Fluid Dyn.* 52:71–87 (1990).
10. M. Stern, Minimal properties of planetary eddies, *J. Mar. Res.* 33:1–13 (1975).
11. Z. Kizner, R. Khvoles, and J. C. McWilliams, Rotating multipoles on the f and γ planes, *Phys. Fluids* 19:016603 (2007).
12. O. U. Velasco Fuentes, Propagation and transport properties of dipolar vortices on a gamma plane, *Phys. Fluids* 6:3341–3352 (1994).
13. O. G. Derzho and R. Grimshaw, Rossby waves on a shear flow with recirculation cores, *Stud. Appl. Math.* 115:387–403 (2005).
14. O. G. Derzho and Y. D. Afanasyev, Rotating dipolar gyres on a gamma-plane, *Phys. Fluids* 20:036603 (2008).
15. J. Pedlosky, *Geophysical Fluid Dynamics* (2nd ed.), Springer, New York, 1986.
16. S. T. Gille, Mean sea surface height of the antarctic circumpolar current from geosat data: Methods and application, *J. Geophys. Res.* 99(C9):18255–18273 (1994).
17. W. M. Connolley, Long term variation of the antarctic circumpolar wave, *J. Geophys. Res.* 108(C4):8076–8098 (2003).
18. E. I. Sarukhanian, *Structure and Variability of the Antarctic Circumpolar Current*, Oxonian Press, New Delhi, 1985.

Memorial University of Newfoundland
Institute of Thermophysics, Russian Academy of Sciences

(Received September 1, 2010)